Enhancement of magnetoresistance in Co(1$\bar{1}$00)/Cr(211) bilayered films on MgO(110)

Y. D. Yao[a] and Y. Liou
Institute of Physics, Academia Sinica, Taipei 115, Taiwan, Republic of China

J. C. A. Huang
Department of Physics, National Cheng Kung University, Tainan 701, Taiwan, Republic of China

S. Y. Liao, I. Klik, W. T. Yang, C. P. Chang, and C. K. Lo
Institute of Physics, Academia, Sinica, Taipei 115, Taiwan, Republic of China

Epitaxial Co/Cr bilayered films have been successfully grown on the MgO(100) and MgO(110) substrates by molecular-beam epitaxy. According to the reflection high-energy electron-diffraction and x-ray-diffraction measurements the crystal structure of the film depends on orientation of the buffer and substrate. Epitaxial growth of biaxial Co(11$\bar{2}$0)/Cr(100) on MgO(100) substrate and of uniaxial Co(1$\bar{1}$00)/Cr(211) on MgO(110) substrate has been confirmed. The anisotropy magnetoresistance (AMR) is strongly influenced by the orientation of the Cr buffer. In Co(11$\bar{2}$0)/Cr(100) on MgO(100) AMR is isotropic for all in-plane fields. However, for Co(1$\bar{1}$00)/Cr(211) on MgO(110) we observed enhancement of AMR along the easy axis for temperatures below 150 K, while along the hard axis AMR has a local maximum at about 150 K. The easy axis data suggest that the longitudinal spin density wave of Cr and the crystal anisotropy of Co on Cr(211) plane dominate the enhancement of the AMR. © *1996 American Institute of Physics.* [S0021-8979(96)57808-1]

In previous studies of the Co/Cr multilayer system[1–3] its magnetoresistance (MR) was shown to be quite small in comparison with other giant MR (GMR) multilayer systems.[4] Recently it was realized[5,6] that the magnetic properties of the Co/Cr multilayer system are sensitive to anisotropy and to the orientation of the applied magnetic field with respect to crystallographic axes and MR as high as 18% as has been observed in the Co/Cr(211) superlattice system. However, the mechanism of this effect is presently not clear and this motivated us to investigate the simpler case of anisotropy of MR (AMR) in the epitaxial bilayered Co/Cr film system.

Epitaxial Co/Cr bilayer films have been simultaneously prepared on MgO(110) and MgO(100) substrates by using an Eiko EL-10A molecular-beam-epitaxy (MBE) system with base pressure of 2×10^{-10} Torr. To enable the growth of high-quality film samples, polished and epitaxial grade MgO(110) and MgO(100) substrates were chemically precleaned and rinsed in an ultrasonic cleaner. They were then outgassed at 900–1000 °C for at least 0.5 h under ultrahigh vacuum in the MBE chamber. High-purity Co and Cr elements (>99.99%) were evaporated from two independent e-beam evaporators. During deposition of the films, the substrate temperature was kept between 300 and 350 °C, the growth pressure was controlled at below 5×10^{-9} Torr, and the deposition rate kept at ~0.1 Å/s. The film thickness and deposition rate were measured by a quartz-crystal thickness monitor. The crystallographic structure of the surface of the films was *in situ* examined throughout the growth by 15 keV reflection high-energy electron diffraction (RHEED). The crystal orientation was *ex situ* characterized by x-ray diffraction (XRD). The magnetic properties of all samples were studied using a superconducting quantum interference device (SQUID) magnetometer. The AMR measurements were carried out by standard four-probe technique in a magnetic field up to 5 T at temperatures ranging between 10 and 300 K. Typical area of the film sample was roughly 1.5×6.0 mm^2.

The structure arrangement of both Co and Cr layers in the Co/Cr bilayered films is considerably affected by the choice of the interface direction of the MgO substrate. In this study, the epitaxial Co/Cr bilayer films were simultaneously grown on MgO(100) and on MgO(110) substrates. Their crystalline orientation and quality were determined by RHEED and XRD. Figures 1(a) and 1(b) show schematic diagrams of the 3D geometry of the Co(1$\bar{1}$00)/Cr(210)/MgO(110) and Co(11$\bar{2}$0)/Cr(100)/MgO(100) bilayer films. These epitaxial relationships were also confirmed by both RHEED and XRD studies. Part of the structural analysis related to the Co/Cr superlattice films will be published elsewhere,[5,6] in this study only the bilayer case is discussed. In Fig. 1(a) the lattices of the Co and Cr layers appear to be rectangular, in acccordance with the 4.21×2.98 Å^2 unit cell of the MgO(110) surface. The unit cell of Co(1$\bar{1}$00), 4.07×2.51 Å^2, matches perfectly that of Cr(211), 4.07×2.50 Å^2, and even though the match between Cr(211) and MgO(110) is poorer, we did experimentally observe a twofold symmetry for the whole system and confirmed that the *c* axis of Co is in the film plane and in the Cr[0$\bar{1}$1] direction only. On the other hand, for the Co(11$\bar{2}$0)/Cr(100)/MgO(100) system, because the bcc Cr(100) plane has fourfold symmetry with unit cell of 2.88×2.88 Å^2, the hcp Co(11$\bar{2}$0) plane possesses only pseudotwofold symmetry with unit cell of 4.34×4.07Å^2. This suggests that the Co(11$\bar{2}$0) layers behave

[a]Also with: Department of Physics, National Chung Cheng University, Chiayi 621, Taiwan, Republic of China.

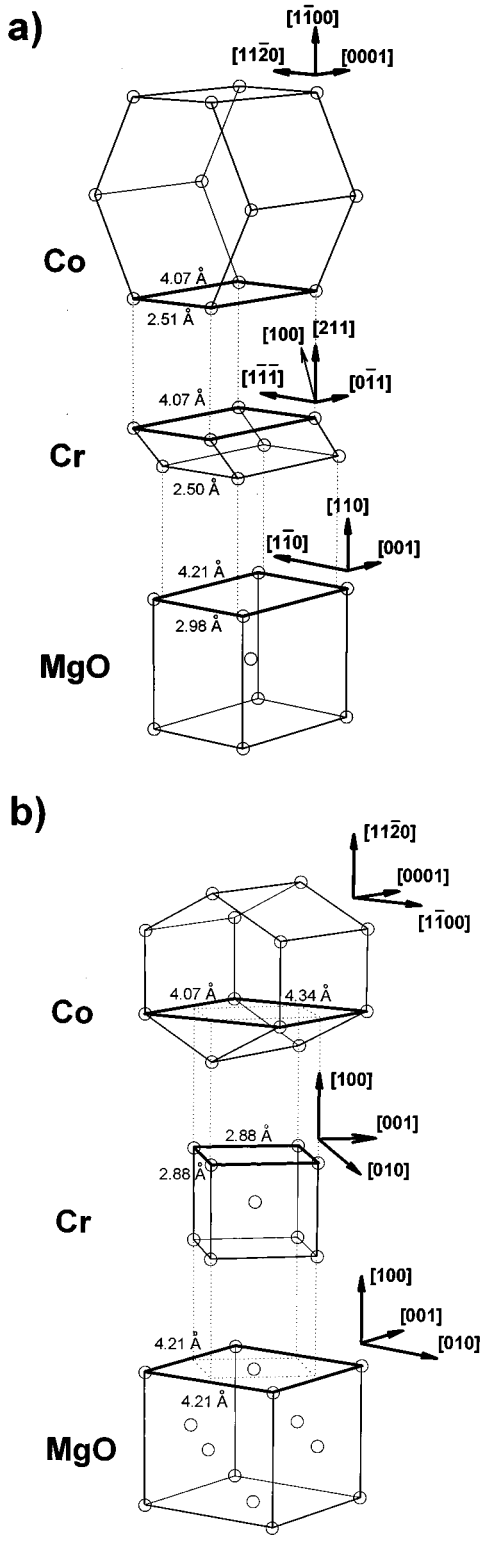

FIG. 1. Schematic diagram of the 3D geometry, unit cell (indicated by bold lines), and epitaxial relationships for (a) Co(1$\bar{1}$00)/Cr(211)/MgO(110) films, and (b) Co(1120)/Cr(100)/MgO(100) films.

like a bicrystalline structure; i.e., that the Co[0001] easy axis can either be parallel to MgO[001] or to MgO[010] as shown in Fig. 1(b).

The thickness of the Co layer for all the samples in this study is fixed at 200 Å and the thickness of the Cr layer is

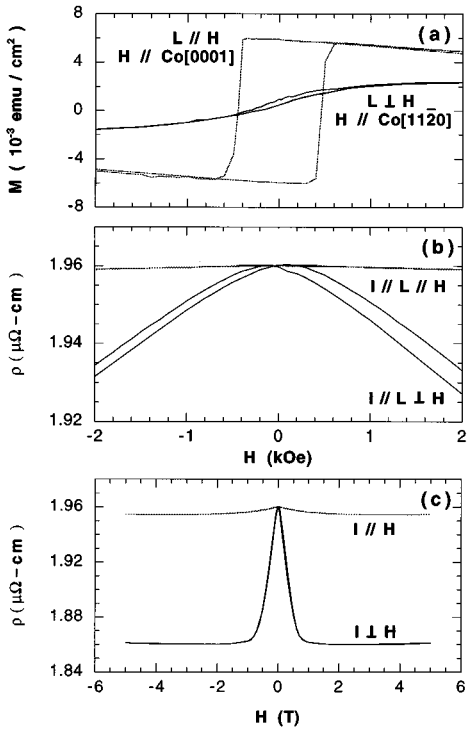

FIG. 2. (a) The magnetization M and (b) and (c) the surface resistivity for $Co_{200\ Å}(1\bar{1}00)/Cr_{6\ Å}(211)/MgO(110)$ films at $T=10$ K as functions of magnetic field applied parallel to the film surface.

varied between 6 and 100 Å. As an example, Fig. 2 shows the magnetic hysteresis loops and the corresponding surface resistivity of the $Co_{200\ Å}(1\bar{1}00)/Cr_{6\ Å}(211)/MgO(110)$ sample at 10 K for field applied parallel to the film surface. For H parallel to the easy axis of the Co layers a square $M-H$ hysteresis loop and small variation of resistivity have been observed. We interpret the magnetization reversal process as being mainly due to domain-wall motion. On the other hand, for H applied parallel to the hard axis of Co layers the magnetization varies slowly with increasing H while electric resistivity decreases very fast below roughly $H=1$ T and saturates then at $H>1$ T. The (very small) values of coercivity deduced from the $M-H$ loop are consistent with the peak positions on the resistivity curve.

In Fig. 3 we plot the magnetization M and surface resistivity as functions of applied field H for a $Co_{200\ Å}(11\bar{2}0)/Cr_{6\ Å}(100)/MgO(100)$ sample at 10 K. According to our structure analysis above, the easy and hard axes of the Co layers are randomly distributed in both MgO[001] and MgO[010] directions. The $M-H$ curves for H applied parallel or perpendicular to the long axis of the sample are roughly the same, apart from a difference due (presumably) to demagnetization factors [see the geometry of Fig. 1(b)]. The coercive force obtained from the $M-H$ curves coincides with the location of a minimum (maximum) of the resistivity with current parallel (perpendicular) to the applied field.

The temperature dependence of the AMR of the saturation magnetization M_S and of the coercive force H_c between 10 and 300 K for both $Co_{200\ Å}/Cr_{6\ Å}/MgO(110)$ and

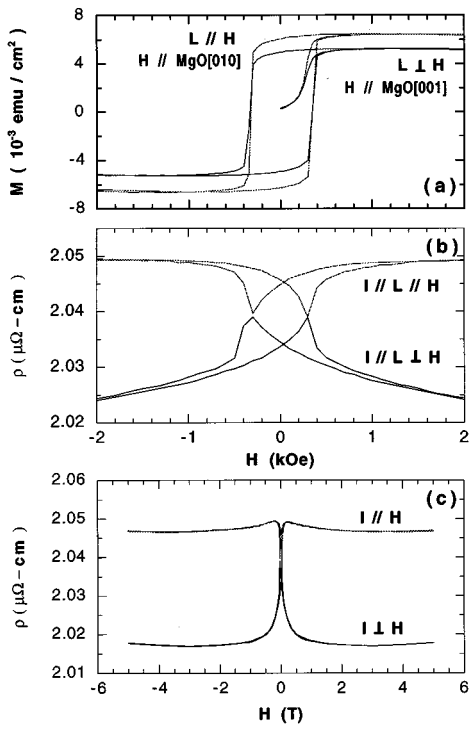

FIG. 3. (a) The magnetization M and (b) and (c) the surface resistivity for $Co_{200\ Å}(11\bar{2}0)/Cr_{6\ Å}(100)/MgO(100)$ films at $T=10$ K as functions of magnetic field applied parallel to the film surface.

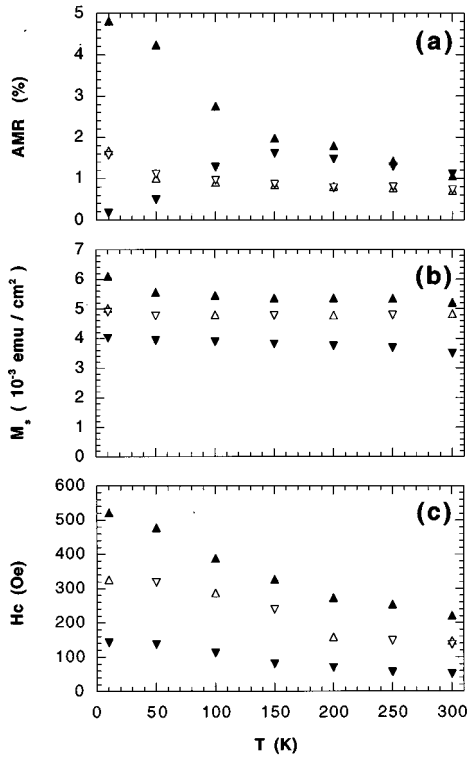

FIG. 4. (a) The AMR, (b) the saturation magnetization, and (c) the coercive force as functions of the temperature between 10 and 300 K for (L: long side of film): (▲) $Co_{200\ Å}/Cr_{6\ Å}/MgO(110)$ with $L\|$ easy axis of Co surface;(▼) $Co_{200\ Å}/Cr_{6\ Å}/MgO(110)$ with $L\|$ hard axis of Co surface; (△) $Co_{200\ Å}/Cr_{6\ Å}/MgO(110)$ with $L\|MgO[001]$ direction; and (▽) $Co_{200\ Å}/Cr_{6\ Å}/MgO(110)$ with $L\|$ MgO[010] direction.

$Co_{200\ Å}/Cr_{6\ Å}/MgO(100)$ are presented in Fig. 4. For samples of $Co_{200\ Å}/Cr_{6\ Å}/MgO(110)$ with their long axis parallel to the easy axis of Co, i.e., in the direction of Co[0001] as shown in Fig. 1(a), we observed a significant enhancement of AMR for temperatures roughly below 150 K [▲ in Fig. 4(a)] while AMR [▼ in Fig. 4(a)] decreases with decreasing temperature below roughly 150 K for samples with long axis parallel to the hard axis of Co, i.e., in the direction of $Co[11\bar{2}0]$ as shown in Fig. 1(a). Our data points between 100 and 150 K are not sufficiently dense, however, this characteristic temperature T_f ($\sim$150 K) may be very close to the spin-flip temperature $T_{sf}=123$ K of Cr and we conjecture that magnetization reversal in these samples may be explained by a mechanism similar to that reported for the Fe/Cr system.[7] By contrast, in $Co_{200\ Å}/Cr_{6\ Å}/MgO(100)$ samples the AMR as shown in Fig. 4(a) is almost independent of temperature. The saturation magnetization M_s and the coercive force H_c as functions of temperature between 10 and 300 K are plotted in Figs. 4(b) and 4(c), respectively. Both the M_s vs T and the H_c vs T curves completely coincide for the $Co(11\bar{2}0)/Cr(100)/MgO(100)$ samples; however, a slight shift in these data, perhaps again explainable by the presence of demagnetizing fields, exists in the observed values for the $Co(1\bar{1}00)/Cr(211)/MgO(110)$ samples. All H_c vs T curves show a marked change in their slope at approximately 150 K.

In conclusion, this is the first time that AMR enhancement roughly below the spin-flip temperature was observed in epitaxial $Co(1\bar{1}00)/Cr(211)$ bilayered films on MgO(110), with current in the Co[0001] direction.

We are grateful for the financial support by the National Science Council of the R.O.C. under Grant Nos. NSC85-2112-M-001-020, NSC85-2112-M-001-019, and NSC85-2112-M-006-006.

[1] S. S. P. Parkin, R. Bhadra, and K. P. Roche, Phys. Rev. Lett. **64**, 2304 (1990).
[2] Y. Liou, J. C. A. Huang, Y. D. Yao, C. H. Lee, K. T. Wu, C. L. Lu, S. Y. Liao, Y. Y. Chen, N. T. Liang, W. T. Yang, C. Y. Chen, and B. C. Hu, J. Appl. Phys. **76**, 6516 (1994).
[3] Y. D. Yao, Y. Liou, J. C. A. Huang, S. Y. Liao, C. H. Lee, K. T. Wu, Y. Y. Chen, C. L. Lu, and W. T. Yang, Chin. J. Phys. **32**, 863 (1994).
[4] M. N. Baibich, J. M. Broto, A. Fert, F. Nguyen van Dau, F. Petroff, P. Etienne, G. Creuzet, and J. Chazelas, Phys. Rev. Lett. **61**, 2472 (1988).
[5] Y. Liou, J. C. A. Huang, Y. D. Yao, S. F. Lee, W. T. Yang, S. Y. Liao, and C. P. Chang, IEEE Trans. Magn. **31**, 3927 (1995).
[6] J. C. A. Huang, Y. Liou, Y. D. Yao, W. T. Yang, C P. Chang, S. Y. Liao, and Y. M. Hu, Phys. Rev. B **52**, R 13 110 (1995).
[7] A. Berger and H. Hopster, Phys. Rev. Lett. **73**, 193 (1994).